Available online at www.sciencedirect.com

jmr&t Journal of Materials Research and Technology

www.jmrt.com.br

Original Article

Effect of Mn addition on Fe-rich intermetallics morphology and dry sliding wear investigation of hypereutectic Al-17.5%Si alloys

Cyrus Bidmeshki[a,*], *Vahid Abouei*[a], *Hassan Saghafian*[b], *Saeed Ghodratnama Shabestari*[b], *Mohammad Talafi Noghani*[c]

[a] *Department of Materials Engineering, Karaj Branch, Islamic Azad University, Karaj, Iran*

[b] *Center of Excellence for High Strength Alloys Technology (CEHSAT), School of Metallurgy and Materials Engineering, Iran University of Science and Technology (IUST), Tehran, Iran*

[c] *Faculty of Engineering and Technology, Department of Materials Engineering, Imam Khomeini International University, Qazvin, Iran*

ARTICLE INFO

Article history:
Received 4 July 2015
Accepted 12 November 2015
Available online 27 January 2016

Keywords:
Al—Si hypereutectic alloys
Mn modification
Intermetallic compounds
Wear behavior
Friction coefficient

ABSTRACT

The effect of Manganese addition on the iron-rich intermetallics and wear behavior of Al-17.5%Si hypereutectic alloys has been studied. Dry sliding wear tests have been conducted using a pin-on-disk machine under different normal loads of 18, 51, 74 and 100 N and at a constant sliding speed of 0.3 m/s. The addition of 1.2 wt.% Fe to the base alloy increased the wear rate due to the formation of needle beta intermetallics. Introducing 0.6 wt.% Mn to the iron-rich alloy changed the beta intermetallics into the modified alpha phases, and therefore reduced the detrimental effect of iron. Mn addition up to 0.9 wt.% to the 1.8Fe alloy did not impede formation of needle-like intermetallic compounds and had no positive effect on the modification of microstructure.

1. Introduction

It is well established that hypereutectic Al—Si cast alloys have the good potential for tribological applications [1,2]. Silicon as a hard material increases the wear resistance of Al—Si hypereutectic alloys [3,4]. The presence of Fe and its compounds can be a problem in hypereutectic Al—Si alloys [5,6]. Iron as an impurity in Al—Si alloys or as necessary element in the die-cast process can leave some serious detrimental effects on the mechanical properties of the casting parts [7]. This is due mainly to the precipitation of brittle β-Al_5FeSi intermetallics that appear as needles or plate-like morphologies in the microstructure [8–10]. However, in Al—Si piston alloys, iron is a desirable element that helps to enhance high temperature properties and thermal stability of the alloy [11,12]. Attempts have to be made to modify the negative effects of iron intermetallics, e.g., by refining their size and by modifying them to the less deleterious morphologies [11]. Alloy chemistry is an important factor that influences the formation of the β-particle. It is well known that trace addition of suitable neutralizer elements like Mn, Cr, Be, Co, and Sr can modify the β-phase morphology to less harmful forms [8–10]. Among these, Mn is an effective element in the modification

* *Corresponding author.*
E-mail: cyrusbidmeshki@gmail.com (C. Bidmeshki).

http://dx.doi.org/10.1016/j.jmrt.2015.11.008

of needle-like intermetallic compounds [13–15]. It has been shown that manganese addition up to the half of the iron amount results to the formation of some Mn-containing intermetallic compounds in the matrix, such as $Al_{15}(Fe,Mn)_3Si_2$ [15]. Taghiabadi et al. [16] have shown that addition of about 0.7 wt.% Fe increased the hardness and improved the wear resistance of the F332 Al—Si alloy. Addition of iron up to 2.5 wt.% increased the hardness, but decreased the wear resistance. It has been shown that the addition of Mn into the iron-containing eutectic Al—Si alloys converts the needle-like β-intermetallics into the well modified α-intermetallic compounds and improves the wear resistance of the alloy [17]. This investigation has been focused on the modification of these iron-rich intermetallics and to study their effects on the dry sliding wear of hypereutectic Al-17.5%Si alloy.

2. Experimental procedure

The composition of hypereutectic Al—Si alloy used in the present study is given in Table 1. In order to investigate the effect of Fe-rich intermetallics on the wear behavior of the alloy, iron and manganese were added to the base alloy in order to obtain 1.2Fe alloy containing 1.2 wt.% Fe, 1.2FeMn alloy containing 1.2 wt.% Fe and 0.6 wt.% Mn and 1.8FeMn alloy containing 1.8 wt.% Fe and 0.9 wt.% Mn (Table 1). Iron and manganese were added to the melt at 750 °C using ALTAB Fe compact (75 wt.% Fe, 15 wt.% Al and 10 wt.% nonhygroscopic Na-free flux) and Mn compact (75 wt.% Mn, 15 wt.% Al, and 10 wt.% nonhygroscopic Na-free flux), respectively. After the additions were made, the temperature of the melt was raised to 800 °C, under covered flux, held for 15 min to homogenize the liquid, then cooled in the furnace to 750 °C. The melt was stirred and degassed using Foseco 600 tablet for 10 min and final pouring temperature was always 720 ± 5 °C. The molten alloys were cast into a copper mold having the average cooling rate of 7.5 °C s^{-1}. The hardness of all samples was measured using a Brinell hardness tester with the load of 31.25 kgf. The effect of alloy chemistry on the microstructure was studied by a TESCAN VEGA2 scanning electron microscope (SEM) equipped with an energy dispersive X-ray spectrometer (EDS). A computer-assisted Buhler Omnimet image analysis system was used to measure the morphological parameters of Fe intermetallics including the length and the volume fraction of iron intermetallic particles. Dry sliding wear experiments were performed using a pin-on-disk machine against the counterface of a hardened and ground (Ra = 0.5 μm) steel disk (diameter 50 mm and 10 mm thickness) with HRC 62–65 hardness. The pin samples, 5 mm × 5 mm, were prepared in the flat contact region by polishing up to 0.5 μm (Ra) and cleaning with acetone to remove dust and grease from the surface. The tests were done in air atmosphere at a relative humidity of 40 ± 2% at room temperature (25 °C). Dry sliding was conducted under normal loads of 18, 51, 74 and 100 N, at a constant sliding speed of 0.3 m s^{-1} for a sliding distance of 1000 m. Each test was repeated three times with identical new samples on fresh disk surface and the weight loss determined as a function of distance was used for the analysis of the wear rate.

3. Results and discussion

3.1. Microstructure and hardness

The microstructure of base alloy is depicted in Fig. 1a. As observed, the base alloy contains complex intermetallics (phase A). The chemical composition of these intermetallics is shown in Table 2. These intermetallics are rich in Ni and Cu due to the presence of these elements in the composition of the base alloy. The addition of iron to the base alloy led to the precipitation of needle-like intermetallic (phase B) in the matrix as shown in Fig. 1b. The average atomic concentrations of Al, Fe and Si were in a good agreement with the concentrations obtained for the β-Al_5FeSi needles by others [18–20]. Fig. 1c shows the microstructure of 1.2FeMn alloy. The addition of Mn up to the half of Fe amount causes the replacement of β needle-like intermetallic by star-like polygonal morphologies (phase C). According to Table 2, the average atomic percentage of the star-like intermetallic is $Al_{15}(Fe,Mn)_3Si_2$ phase, which is in a good agreement with what was previously reported [21]. Fig. 1d shows the effect of 1.8 wt.% Fe and 0.9 wt.% Mn addition on the microstructure of 1.8FeMn alloy. As can be seen, exceeding amount of iron up to 1.8% in the 1.8FeMn alloy despite the presence of manganese leads to the formation of needle-like and cubic intermetallic compounds (phase D), which have blade nature in the matrix in fact. Chemical composition analysis of these compounds did not illustrate β-Al_5FeSi and α-$Al_{15}(Fe,Mn)_3Si_2$ phases in the microstructure. Instead confirmed that chemical composition of this phase was similar to $Al_4(Fe,Mn)Si_2$ intermetallic compounds. These intermetallic particles are called δ phase. The image analysis results of the volume fraction and the average maximum size of the intermetallic phases are presented in Table 3. It demonstrates that the size and the volume fraction of intermetallic compounds in 1.8FeMn alloy have increased 59.71% and 3.41%, respectively, compared to those observed in 1.2FeMn alloy. Table 3, also shows the Hardness of alloys investigated in the present study. It is observed that the addition of 1.2 wt.% Fe to the base alloy increased the hardness from 115 ± 0.91 HB to 121 ± 0.65 HB. The hardness of 1.2FeMn alloy (122 ± 0.71 HB) is approximately equal to that of 1.2Fe alloy, while the 1.8FeMn alloy has higher hardness value (130 ± 0.23 HB) in the microstructure compared to the other alloys.

Table 1 – Designations and chemical compositions of the hypereutectic Al—Si alloys (wt.%).

Alloy code	Si	Cu	Ni	Mg	Zn	Fe	Mn	Al
Base	17.54	1.02	1.11	0.95	0.017	0.42	–	Balance
1.2Fe	17.81	1.05	0.91	0.98	0.018	1.15	0.53	Balance
1.2FeMn	17.44	0.88	1.09	0.91	0.018	1.22	0.63	Balance
1.8FeMn	17.61	0.95	1.02	0/92	0.013	1.81	0.79	Balance

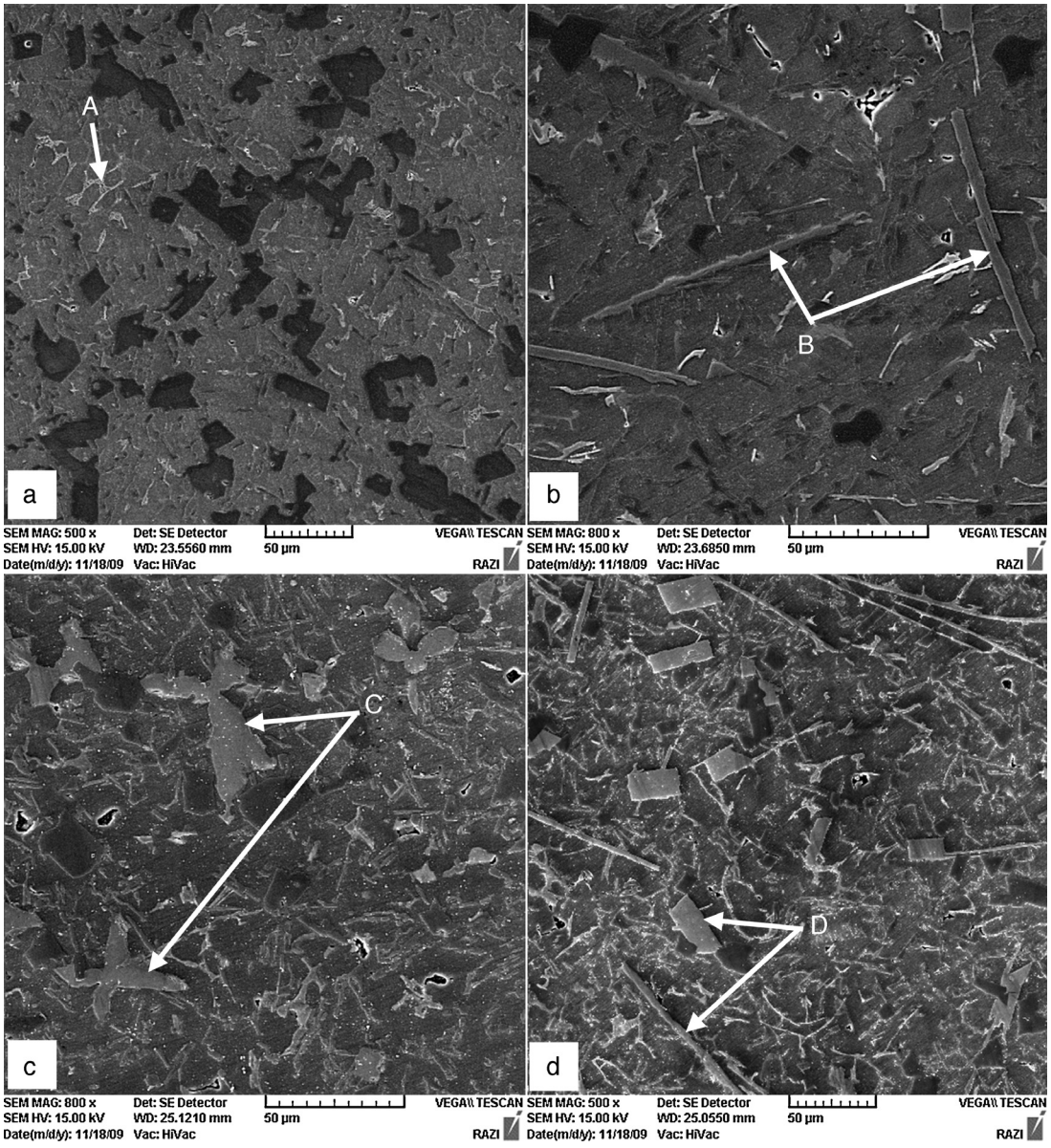

Fig. 1 – Microstructures of the (a) base alloy, (b) 1.2Fe alloy, (c) 1.2FeMn alloy and (d) 1.8FeMn alloy.

Table 2 – Chemical composition of the phases shown in the micrographs of Fig. 1 (at.%).

Alloy code	Phases	Morphology	Atomic percentage					
			Al	Si	Fe	Mn	Cu	Ni
Base alloy	A	–	73.28	4.38	2.84	–	4.47	15.03
1.2Fe	B	Needle-like	67.08	16.45	15.77	–		0.6
1.2FeMn	C	Star-like	71.84	10.39	11.04	5.76		0.3
1.8FeMn	D	Needle-like and Cubic	72.98	9.57	10.37	6.57	–	

Table 3 – Hardness, volume fraction, and the average maximum size of Fe-rich intermetallic phases.

Alloy code	Hardness	Morphology	Volume fraction of phase (%)	Average maximum size of the phase (μm)
Base alloy	–	115 ± 0.91	–	–
1.2Fe	Needle-like	121 ± 0.65	11.90 ± 7.32	55.31 ± 18.51
1.2FeMn	Star-like	122 ± 0.71	13.90 ± 6.19	38.79 ± 17.60
1.8FeMn	Needle-like Cubic	130 ± 0.23	17.31 ± 8.20	70.2 ± 32.11 28.3 ± 11.22

3.2. *Wear characterizations*

Fig. 2 displays the effect of Fe and Mn parameters on the wear rate of base alloy at the applied loads of 18, 51, 74, and 100 N. It can be observed that the addition of 1.2% Fe to the base alloy creates a detrimental effect on the wear behavior of the alloy. The 1.2Fe alloy has the highest wear rate compared to the base alloy at all applied loads. Fig. 2 shows that the addition of Mn to the 1.2Fe alloy declines the detrimental effects of iron and improves the wear rate of 1.2FeMn alloy compared to that of 1.2Fe alloy. It can be seen that the addition of 0.9% Mn to the 1.8Fe alloy does not decrease the deleterious effects of iron, and consequently it does not help reduce the wear rate of 1.8FeMn alloy compared to that of 1.2FeMn. In hypereutectic Al–Si alloys containing high percentages of silicon, the presence of approximately more than

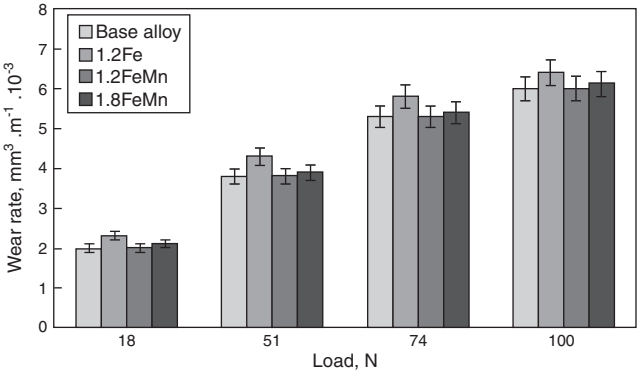

Fig. 2 – Variation of wear rate versus applied load for different alloys.

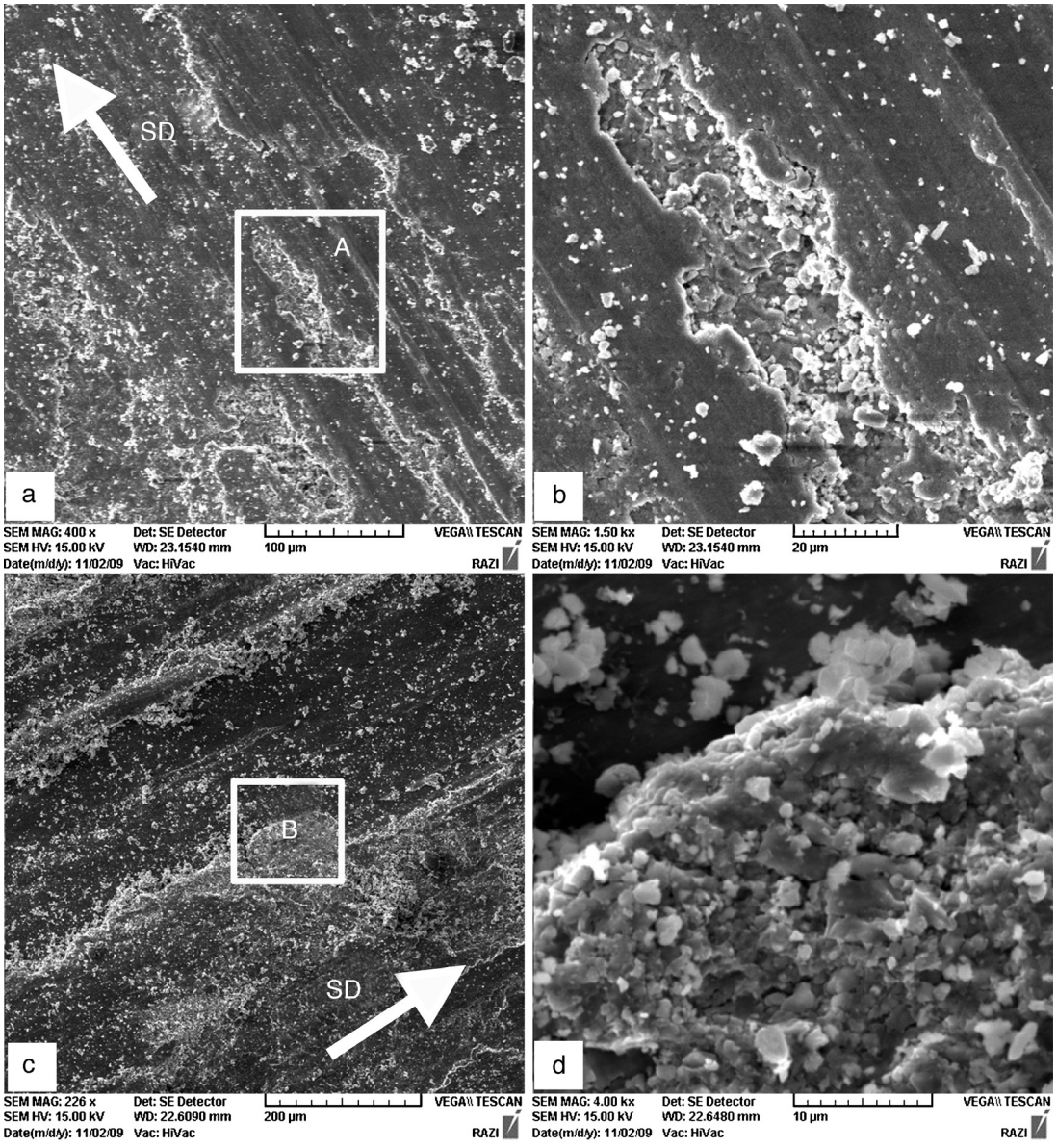

Fig. 3 – SEM micrographs of worn surfaces of (a) base alloy at applied loads of 51 N, (b) enlarged view of the marked region (A) in the micrograph (a), (c) 1.2FeMn alloy at applied loads of 74 N, (d) enlarged view of the marked region (B) in the micrograph (c) (*SD is sliding direction).

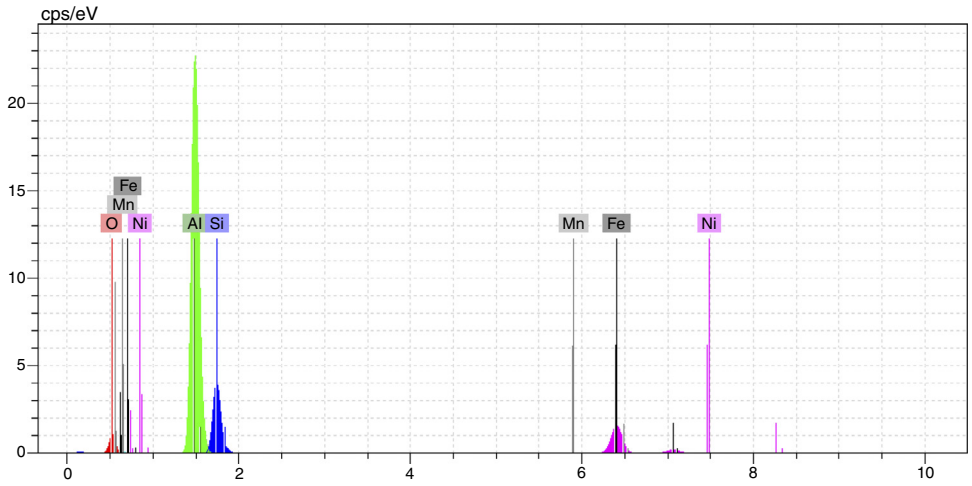

Fig. 4 – EDS result of the worn surface of base alloy at the applied load of 51 N.

1.5% Fe leads to the formation of needle-like and cubic δ-$Al_4(Fe,Mn)Si_2$ intermetallic compounds, and thus, further Mn addition to alloy composition cannot result to the formation of modified α-$Al_{15}(Fe,Mn)_3Si_2$ intermetallic compounds and decrease the deleterious effects of iron [21]. The higher wear rate of the 1.8FeMn alloy compared to the 1.2FeMn alloy is due to existence of needle-like intermetallic compounds and more potential to formation of microcracks in the subsurface of the alloy. The SEM micrographs of the worn surfaces of the base alloy and 1.2FeMn alloy are shown in Fig. 3. Fig. 3a shows that the worn surface was mostly covered by some particles under applied load of 51 N. These particles formed on the worn surface of the pin contained a certain amount of iron, aluminum, silicon and oxygen as examined by EDS in Fig. 4. Based on the compositional analysis, it can be concluded that much of the wear debris is composed of oxide particles. These oxide particles could become entrapped between the sliding surfaces and get compacted due to the repetitive sliding. Then they form a tribolayer over the surface, as shown in Fig. 3d. Fig. 5 shows the subsurface micrographs of the base, 1.2Fe, 1.2FeMn and 1.8FeMn alloy at the applied load of 51 and 74 N. During sliding, high tangential stresses take place at the sliding surface, resulting in nucleation of cracks within the plastically deformed material, beneath the surface [22–24], as shown in Fig. 5a. The cracks can be propagated and their connection to each other can lead to delamination of metallic and intermetallic particles from the surface. These fragmented metallic particles could be mechanically mixed with the oxides in the contact zone and form a tribolayer (MML), as shown in Fig. 5b and c. The stresses derived on the surface during sliding can weaken the tribolayer and lead to the delamination and fracture of oxide film generated through the wear debris (Fig. 6a). According to Fig. 7, the wear debris of base alloy, contained a certain amount of iron, aluminum and oxygen that is similar to what observed in the worn surfaces of the alloys in Fig. 4, although there appears to be a bit more aluminum in the wear debris (Fig. 4). The reduction in wear resistance of 1.2Fe alloy compared to the base alloy, as shown in Fig. 2, can be explained based on the microstructural features of the alloys. Fig. 1b shows that addition of iron to the base alloy led to the precipitation of β-phase intermetallic in the matrix. β-Al_5FeSi needle-like intermetallics are hard and brittle phases. They exist as discrete particles with a highly faceted nature in the alloy matrix [25,26]. Accordingly, it has relatively low bond strength with the matrix and the interfacial regions between this phase and the matrix become quite prone to microcracking [27]. Moreover, sharp edges of the β-needles introduce severe stress concentrations in the matrix of the alloy [21]. According to Fig. 2 the enhancement in the wear resistance of 1.2FeMn and compared to 1.2Fe can be originated from the replacement of β-needle-like intermetallics by the modified α-intermetallic compounds. Since the α-intermetallics have a modified morphology rather than the needle-like β phase, they have little effect on the formation of surface and subsurface microcracks. Also, the α-intermetallics form a rough interface with the matrix and their better bonding with matrix reduces the possibility of crack formation in the interface of intermetallic compounds with the matrix. Fig. 1d shows that the addition of manganese to the 1.8Fe alloy led to the formation of δ-phase intermetallic in the matrix. The blade nature of these intermetallic compounds increased wear rate of the 1.8FeMn alloy, but its wear rate rose up very little compared to the base alloy because some needle-like intermetallics are replaced by modified intermetallics due to the addition of Mn. Also, this phenomenon may have occurred due to hardness enhancement as a result of the formation of the more volume fraction of intermetallic compounds and also the presence of cubic compounds. As, equality of proportion of wear rate in the 1.8FeMn alloy in comparison with the base alloy, shows decline of negative effects of intermetallic compounds, even in the case of the presence of blade intermetallic compounds in the alloy. According to Table 3, the hardness of the alloys from base one to 1.8FeMn alloy illustrates linear increment, whereas wear rate of the alloys from base one to 1.8FeMn alloy follows approximately a sinusoidal procedure that its climax occurs in 1.2Fe alloy. This implies, although hardness values are effective on the wear resistance of hypereutectic Al—Si alloys, microstructure and morphology

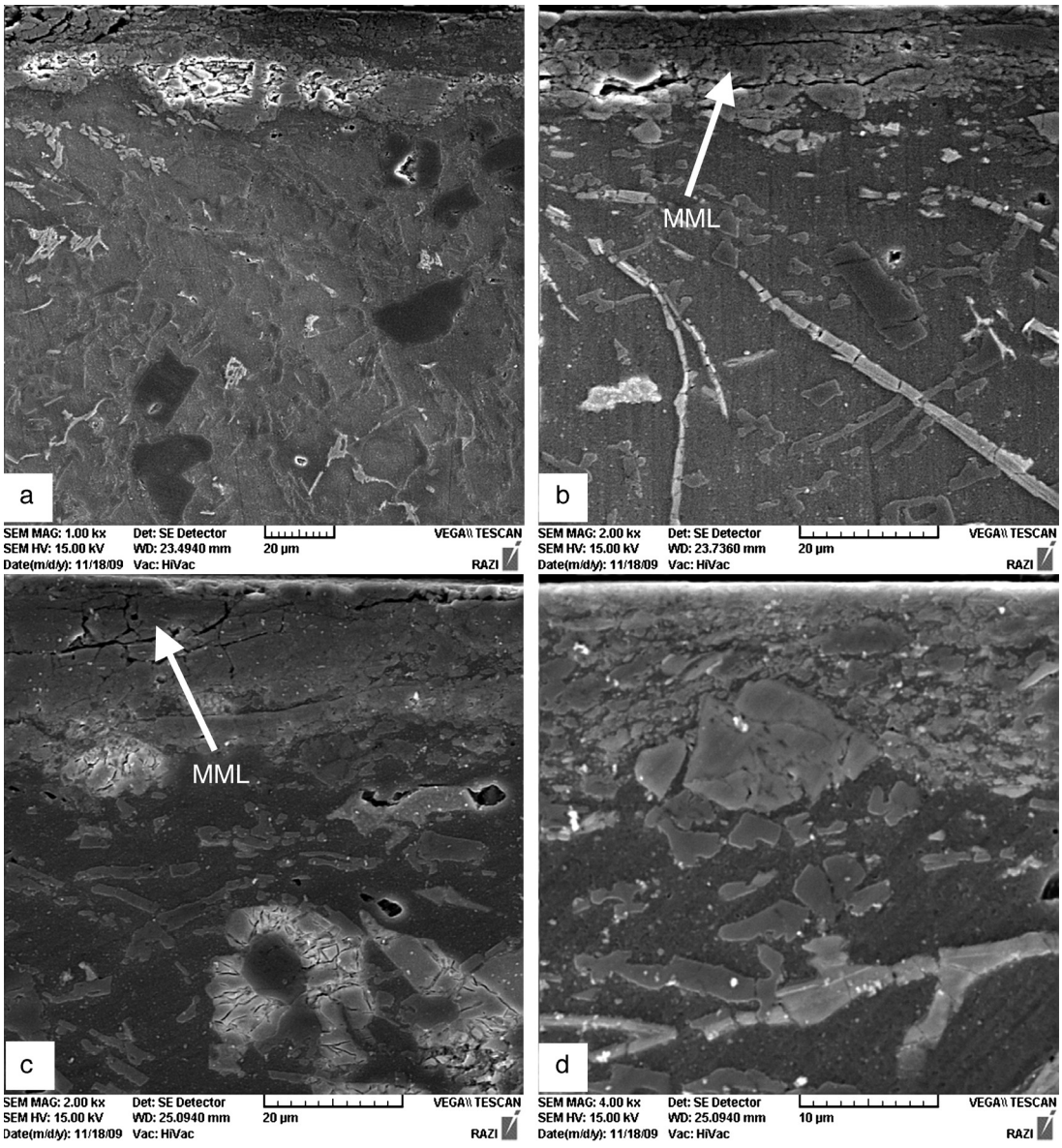

Fig. 5 – (a) Longitudinal cross-section of the worn surface of base alloy at the applied load of 51 N, (b) 1.2Fe alloy at the applied load of 74 N, (c) 1.2FeMn alloy at the applied load of 74 N and (d) 1.8FeMn alloy at the applied load of 74 N.

resulted from the chemical composition and casting process, play substantial role on the wear resistance of hypereutectic Al–Si alloys. According to Fig. 2 the addition of 1.8% Fe and 0.9% Mn to the base alloy led to the increasing of wear rate of 1.8FeMn alloy. The reason for this, as it is clear in Fig. 5d, is mainly due to stress concentration enhancement and crack formation as a result of the presence of needle-like intermetallic compounds [14]. Increasing percentage of iron to about 1.8% led to the formation of needle-like intermetallics neighboring cubic particles and this issue due to stress concentration and tendency of needle-like particles to microcracking would resulted in decrease of wear resistance in the alloy. Lowering wear resistance of hypereutectic alloys containing intermetallic compounds, in addition to alloy trend to crack formation and fracture and segregation of intermetallic compounds, can be considered as alloy brittleness increment owing to intermetallic compounds formation in the alloy structure.

3.3. *Friction coefficient*

Fig. 8 shows the variation of friction coefficient with sliding distance for 1.2FeMn alloy at the load of 51 N. It is noted that the obtained friction coefficient curve is divided into two separated stages. The friction coefficient had little fluctuation and lower coefficient value in the first stage compared to the second one. At longer sliding distances, corresponding to the second segment, the friction coefficient increases and showed greater fluctuation. The coefficient of friction of the 1.2FeMn alloy at the loads of 18 N and 74 N are compared with each other in Fig. 9. It is seen that at the initial distances of sliding the friction coefficient at the load of 18 N has

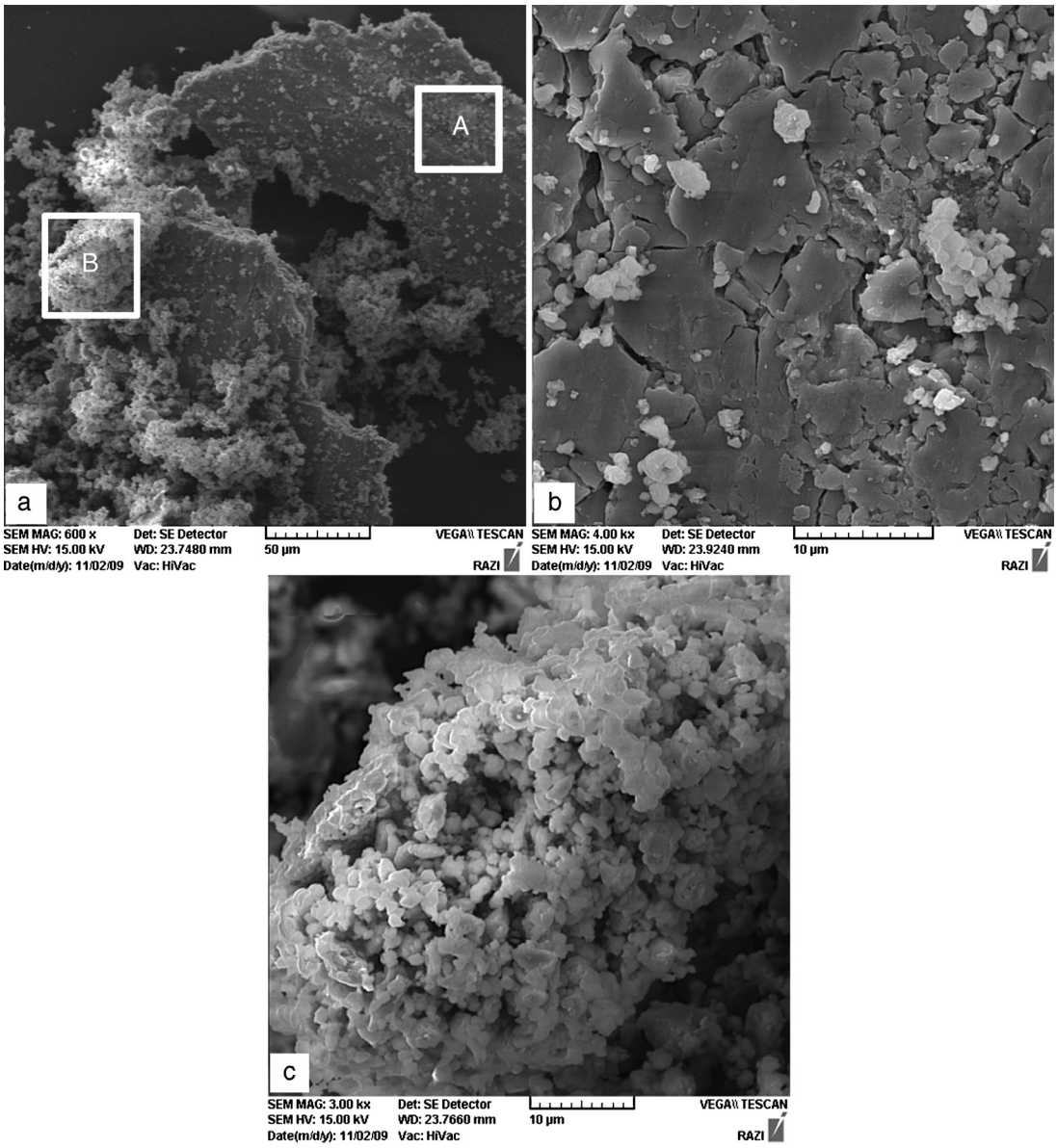

Fig. 6 – (a) SEM micrographs of wear debris of base alloy at the applied loads of 74 N, (b) enlarged view of the marked region (A) in the micrograph (a), (c) enlarged view of the marked region (B) in the micrograph (a).

higher values in comparison with 74 N load, but after continuing sliding the friction coefficient at the load of 74 N increases and has bigger values in comparison with the load of 18 N at the high distances of sliding. According to Fig. 8, in the first stage, small values and less fluctuation of friction coefficient is probably related to the oxide layer formation and prevention of metal-metal contact during sliding [28]. With starting wear and consequently temperature increment between worn surfaces, oxidation of trapped metallic particles fall out and form a thin oxide layer between the sample and counterface so prevent direct metal-metal contact. The prevention of direct metal-metal contact due to the reduction of metallic surfaces, adhesion and lubrication properties of oxide layer led to the decreasing of friction coefficient and observed fluctuations. By increasing sliding distance, sliding intermittent stresses led to the instability and disparting of initial protective oxide layer, and this increases the friction coefficient of mating materials (second stage of curve in Fig. 8) [1,29]. Fig. 9 illustrates friction coefficient of 1.2FeMn alloy at the loads of 18 N and 74 N. As can be observed, friction coefficients for both applied loads have approximately low levels at initial sliding distances (approximately 300 m), whereas, by increasing sliding distance, friction coefficient values in both applied loads increase and demonstrate elevated oscillations. According to Fig. 8, after initial 300 m distance, friction coefficient of 74 N load has higher quantity in proportion to friction coefficient of 18 N load. The reason for this is that at elevated applied loads severe wear mechanism is activated [1], while at the load of 18 N, mild wear is dominant and this led to the low coefficient of friction at this load [22].

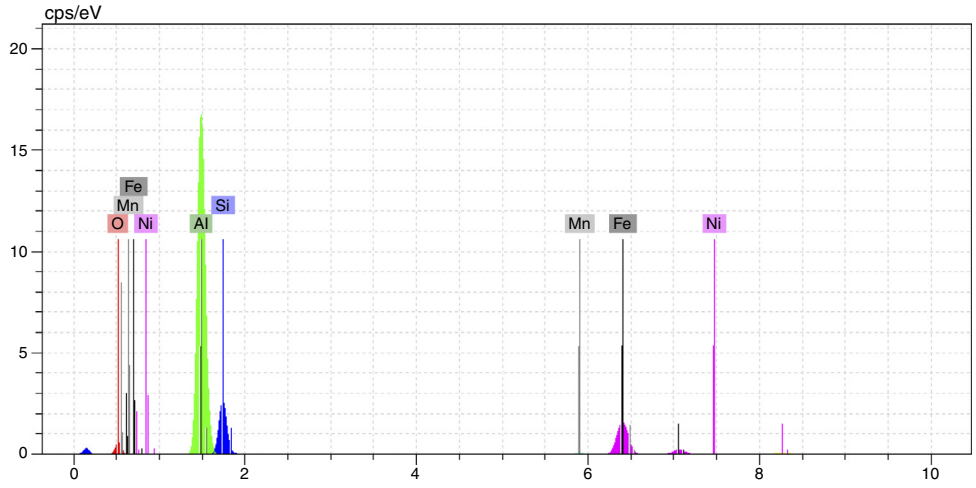

Fig. 7 – EDS result of the wear debris of base alloy at the applied load of 74 N.

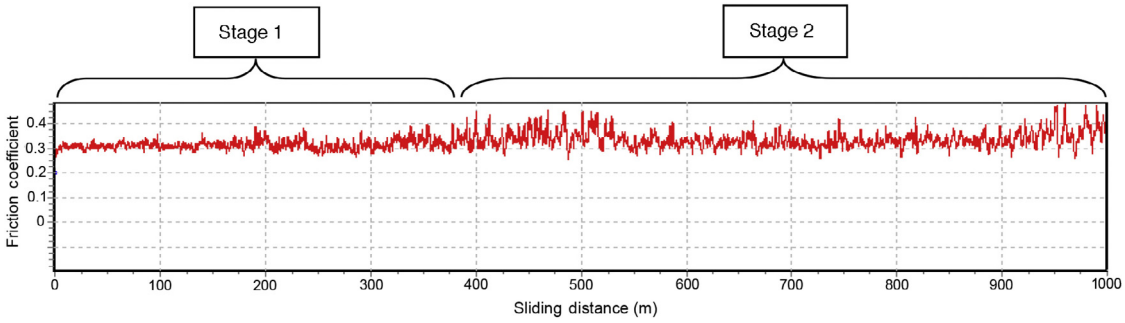

Fig. 8 – Variation of friction coefficient with sliding distance at the load of 51 N in 1.2FeMn alloy.

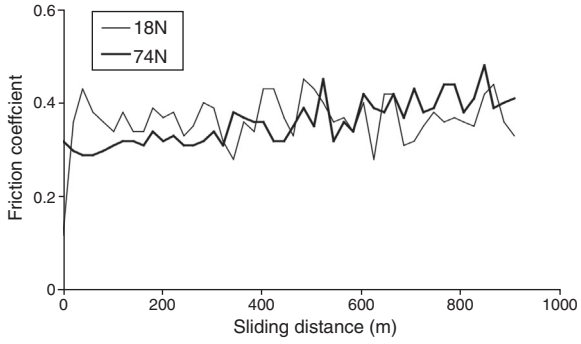

Fig. 9 – Variation of friction coefficient with sliding distance at the loads of 18 N and 74 N in 1.2FeMn alloy.

4. Conclusion

(1) The addition of iron to the hypereutectic Al—Si alloys resulted in the formation of needle-like iron-rich intermetallics in the matrix.
(2) The Mn addition to the alloys containing 1.2 wt.% Fe results in the reduction of the detrimental effect of iron due to the formation of modified alpha intermetallic compounds and increases wear resistance of the 1.2FeMn alloy.
(3) The wear rate of the 1.8FeMn alloy, despite the presence of needle-like phases in the microstructure, is lower than the 1.2Fe alloy due to the higher hardness of the alloy.
(4) The addition of Mn to the alloys containing approximately higher than 1.5 wt.% Fe has no significant effect on the modification of microstructure and does not prevent formation of needle-like intermetallic compounds.

Conflicts of interest

The authors declare no conflicts of interest.

REFERENCES

[1] Henry SD. ASM handbook: friction, lubrication, and wear technology, vol. 18. Ohio: ASM Int.; 1992.
[2] Jasim KM, Dwarakadasa ES. Wear in Al-Si alloys under dry sliding conditions. Wear 1987;119:119–30.
[3] Warmuzek M. Aluminium–silicon casting alloys: atlas of microfractographs. Ohio: ASM Int.; 2004.
[4] Mahato A, Xia S, Perry T, Sachdev A, Biswas SK. Role of silicon in resisting subsurface plastic deformation in tribology of aluminium–silicon alloys. Tribol Int 2010;43:381–7.
[5] Mbuya TO, Odera BO, Nganga SP. Influence of iron on castability and properties of aluminium silicon alloys: literature review. Int J Cast Met Res 2003;16:1–15.

[6] Gruzleski JE, Closet BM. The treatment of liquid aluminium–silicon alloys. Illions: AFS; 1990.
[7] Wang L, Makhlouf MM, Apelian D. Aluminium die casting alloys. Massachusetts: Aluminium Casting Research Laboratory, Worcester Polytechnic Institute; 1993.
[8] Gupta SP. Intermetallic compound formation in Fe–Al–Si ternary system: Part I. Mater Charact 2002;49:269–91.
[9] Huran M, Talib IA, Daud AR. Effect of element additions on wear property of eutectic aluminium–silicon alloys. Wear 1996;194:54–9.
[10] Shabestari SG, Ghodrat S. Assessment of modification and formation of intermetallic compounds in aluminum alloy using thermal analysis. J Mater Sci Eng A 2007;467:150–8.
[11] Mondolfo LF. Aluminum alloys: structure and properties. London: Butterworth; 1978.
[12] Ye H. An overview of the development of Al–Si-Alloy based material for engine applications. J Mater Eng Perform 2003;12:288–97.
[13] Murali S, Raman KS, Murthy KSS. The formation of β-Fe-$SiAl_5$, and Be–Fe phases in Al-7Si-0.3Mg alloy containing Be. Mater Sci Eng A 1995;190:165–72.
[14] Mulazimoglu MH, Zaluska A, Gruzleski JE, Paray F. Electron microscope study of Al–Fe–Si intermetallics in 6201 aluminum alloy. Metall Mater Trans 1996;27A:929–36.
[15] Shabestari SG, Mahmudi M, Emamy M, Campbell J. Effect of Mn and Sr on intermetallics in Fe-rich eutectic Al–Si alloy. Int J Cast Met Res 2002;15:17–24.
[16] Taghiabadi R, Ghasemi HM, Shabestari SG. Effect of iron-rich intermetallics on the sliding wear behavior of Al–Si alloys. Mater Sci Eng A 2008;490:162–70.
[17] Abouei V, Saghafian H, Shabestari SG, Zarghami M. Effect of Fe-rich intermetallics on the wear beheaviour of eutectic Al–Si piston alloy (LM13). J Mater Des 2010;31:3518–24.
[18] Maitra T, Gupta SP. Intermetallic compound formation in Fe–Al–Si turnery system: part II. Mater Charact 2002;49:293–311.
[19] Tash M, Samuel FH, Mucciardi F, Doty HW. Effect of metallurgical parameters on the hardness and microstructural characterization of as-cast and heat-treated 356 and 319 aluminum alloys. Mater Sci Eng A 2007;443:185–201.
[20] Warmuzek M, Ratuszek W, Sek-Sas G. Chemical inhomogeneity of intermetallic phases precipitates formed during solidification of Al–Si alloys. Mater Charact 2005;54:31–40.
[21] Shabestari SG. The effect of iron and manganese on the formation of intermetallic compounds in Al–Si alloys. Mater Sci Eng A 2004;383:289–98.
[22] Abouei V, Saghafian H, Kheirandish Sh. Effect of microstructure on the oxidative wear behaviour of plain carbon Steel. Wear 2007;262:1225–31.
[23] Abouei V, Saghafian H, Kheirandish Sh. An investigation of the wear behaviour of 0.2% C dual phase steels. J Mater Process Technol 2008;203:107–12.
[24] Shabestari SG, Gruzleski JE. The effect of solidification condition and chemistry on the formation and morpholgy of complex intermetallic compounds in aluminum–silicon alloys. Int J Cast Met Res 1994;6:217–24.
[25] Belov NA, Aksenov AA. Iron in aluminum alloys. Impurity and alloying element. New York: Taylor and Francis; 2002.
[26] Ashtari P, Tezuka H, Sato T. Modification of Fe-containing intermetallic compounds by K addition to Fe-rich AA319 aluminum alloys. Mater Trans 2003;44:2611–6.
[27] Shibata S, Tomida S, Nakata K, Light Met. Modification of microstructure and mechanical property of hypereutectic Al–Si alloy by laser surface remelting. J Jpn Inst Light Met 2000;50:609–13.
[28] Cao X, Campbell J. Effect of precipitation and sedimentation of primary α-phase on liquid metal quality of cast Al-11.1Si-0.4Mg alloy. Int J Cast Met Res 2004;17:1–11.
[29] Hutchings IM. Tribology: friction and wear of engineering materials. Cambridge, London: Edward Arnold; 1992.